

MIXED FINITE VOLUME METHOD FOR ELLIPTIC PROBLEMS ON NON-MATCHING MULTI-BLOCK TRIANGULAR GRIDS

YANNI GAO, JUNLIANG LV*, AND LANHUI ZHANG

Abstract. This article presents a mixed finite volume method for solving second-order elliptic equations with Neumann boundary conditions. The computational domains can be decomposed into non-overlapping sub-domains or blocks and the diffusion tensors may be discontinuous across the sub-domain boundaries. We define a conforming triangular partition on each sub-domains independently, and employ the standard mixed finite volume method within each sub-domain. On the interfaces between different sub-domains, the grids are non-matching. The Robin type boundary conditions are imposed on the non-matching interfaces to enhance the continuity of the pressure and flux. Both the solvability and the first order rate of convergence for this numerical scheme are rigorously proved. Numerical experiments are provided to illustrate the error behavior of this scheme and confirm our theoretical results.

Key words. Mixed finite volume method, error estimate, multi-block domain, non-matching grids.

1. Introduction

Let Ω be a bounded polygonal domain in \mathbb{R}^2 with the boundary $\partial\Omega$. Consider the following single phase flow model for the pressure p and the velocity \mathbf{u} :

$$\begin{aligned} (1) \quad & \mathbf{u} = -K(\mathbf{x})(\nabla p - \boldsymbol{\beta}(\mathbf{x})p) && \text{in } \Omega, \\ (2) \quad & c(\mathbf{x})p + \nabla \cdot \mathbf{u} = f && \text{in } \Omega, \\ (3) \quad & \mathbf{u} \cdot \mathbf{n} = 0 && \text{on } \partial\Omega. \end{aligned}$$

Here \mathbf{n} is the outward unit normal vector with respect to $\partial\Omega$, the coefficient $K(\mathbf{x})$ is a symmetric and uniformly positive-definite matrix representing the permeability divided by the viscosity, $\boldsymbol{\beta}(\mathbf{x})$ is a vector representing gravity effect, $c(\mathbf{x}) > 0$ represents the compressibility of the medium, and f is a source or sink term. In many applications, due to the complexity of the domain geometry or the solution itself, the computational domain Ω is required to be a multi-block domain with grids defined independently on each block. Just as introduced in [19, 20], there are two such examples. One is the modeling of flow in a porous medium with known faults [24], in which material properties would have discontinuity. Another one is the modeling of wells, whose solutions are more desired to be carried out on locally refined grids.

In the numerical simulation of (1)-(3) defined on a multi-block domain, each block is independently covered by a local grid and the standard mixed finite element(MFE) methods could be used within each block. However, since grids do not match on the interfaces between different blocks, the normal trace of the velocity space is no longer continuous across these interfaces. In order to overcome this obstacle, several efficient techniques have been developed to enhance the continuity of the pressure and flux. In [20], the MFE method with mortar elements is presented, in which a mortar finite element space is introduced to approximate the

Received by the editors April 4, 2016 and, in revised form, March 22, 2017.

2000 *Mathematics Subject Classification.* 65N08, 65N12, 65N15.

*Corresponding author. *E-mail:* lvjl@jlu.edu.cn.

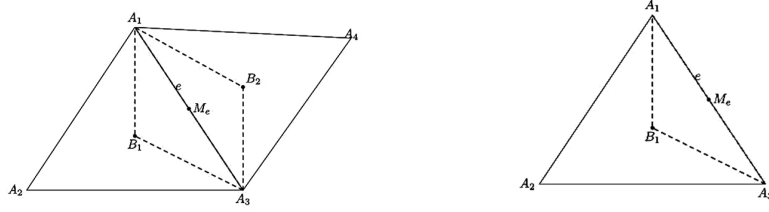
trace of the pressure on the non-matching interfaces, and a continuity condition of the flux is also imposed weakly. This method is optimally convergent if the mortar finite element space has one order higher approximability than the normal trace of the velocity space. In [19], the authors constructed a non-mortar MFE method by imposing Robin type conditions on the non-matching interfaces to unite the sub-domain problems. This method could achieve optimal convergent rate for both the pressure and the velocity, and is more convenient for locally refined grids. Both forementioned methods have to solve interface problems resulting from the additional flux-matching conditions. In [10], the authors studied an alternative approach based on enhancing the velocity space along the sub-domain interfaces. The characteristic of this construction is that it yields a flux-continuous velocity space, and thus no interface problems are required to be solved. These three methods have their respective advantages and have been extended to other different physical and numerical models. Readers are referred to [14, 1, 3, 18, 21, 5] and references therein for their recent developments.

Finite volume(FV) methods have been one class of the most commonly used numerical methods for solving partial differential equations in practice, because they can keep a certain conservation property and have flexibility in handling complicated domain geometries and boundary conditions. On the other hand, it could lead to a better numerical treatment on the velocity by discretizing the equations (1)-(3) directly than just computing it from the pressure. Motivated by these reasons, mixed finite volume(MFV) methods have been proposed and analyzed in [15, 16, 17, 6, 25, 7, 8, 9, 22, 2, 23]. However, their construction and corresponding theoretical analysis are all executed on matching grids. In this article we consider MFV approximation of equations (1)-(3) on non-matching triangular grids. Assume that Ω is a union of non-overlapping polygonal blocks, each covered by a conforming triangular grid. On each block, we employ the standard MFV method based on the lowest order Raviart-Thomas space to discretize equations (1)-(3). On the interfaces between different blocks we use the same technique as that investigated in [19] to keep the continuity of the pressure and flux. The Robin type conditions are imposed weakly on the non-matching interfaces by using double-valued Lagrange multipliers to approximate the trace of the pressure. Since the normal components of the velocity space are no longer continuous across the non-matching interfaces and the term related to Lagrange multipliers also needs to be estimated, it is difficult to extend the theoretical analysis used in the standard MFV method on matching grids to this numerical scheme. Under proper assumptions about the regularity of exact solutions, we give the solvability and convergence analysis of this MFV method on non-matching grids by the main ideas employed in [19]. But some details are quite different.

The rest of the paper is organized as follows. In the next section we introduce some necessary notations, assumptions and definitions. Section 3 is devoted to formulating the MFV method on non-matching multi-block triangular grids and presenting several lemmas which are indispensable in the theoretical analysis. Then, we prove error estimates in Section 4. In Section 5, several numerical examples are presented to test the computational efficiency of this numerical scheme and confirm our theoretical results. Finally, we draw a brief conclusion in Section 6.

2. Preliminaries

We assume that Ω can be divided into non-overlapping sub-domains $\Omega_i, i = 1, 2, \dots, n$, i.e. $\Omega = \bigcup_{i=1}^n \Omega_i$. Let $\Gamma_i = \partial\Omega_i \setminus \partial\Omega$, $\Gamma_{ij} = \partial\Omega_i \cap \partial\Omega_j$ and $\Gamma = \bigcup_{i=1}^n \Gamma_i$



1.a Dual element associated to interior edge e . 1.b Dual element associated to boundary edge e .

FIGURE 1. Primal and dual domains.

be the interior block interface for a given block, the interface between any two sub-domains and the union of all such interfaces, respectively. Particularly, we let $\Gamma_{ii} = \emptyset$.

For the sake of simplicity, we denote $p|_{\Omega_i}$ or its trace $p|_{\Gamma_i}$ by p_i . Let $(\cdot, \cdot)_i$, $\langle \cdot, \cdot \rangle_i$, and $\langle \cdot, \cdot \rangle_{ij}$ have the meaning of $L^2(\Omega_i)$ or $(L^2(\Omega_i))^2$ inner product, interface inner product on $L^2(\Gamma_i)$, and interface inner product on $L^2(\Gamma_{ij})$, respectively. Similarly, (\cdot, \cdot) denotes the $L^2(\Omega)$ or $(L^2(\Omega))^2$ inner product.

Define function spaces:

$$H_0(\text{div}; \Omega) = \{\mathbf{v} \in (L^2(\Omega))^2 : \nabla \cdot \mathbf{v} \in L^2(\Omega), \mathbf{v} \cdot \mathbf{n} = 0 \text{ on } \partial\Omega\},$$

and

$$H_0(\text{div}; \Omega_i) = \{\mathbf{v} \in (L^2(\Omega_i))^2 : \nabla \cdot \mathbf{v} \in L^2(\Omega_i), \mathbf{v} \cdot \mathbf{n} = 0 \text{ on } \partial\Omega_i\}.$$

Then, the associated weak formulation of the first-order system (1)-(3) is: Find $(\mathbf{u}, p) \in H_0(\text{div}; \Omega) \times L^2(\Omega)$ such that

$$\begin{aligned} (K^{-1}(\mathbf{x})\mathbf{u}, \mathbf{v}) &= (p, \text{div}\mathbf{v}) + (\boldsymbol{\beta}(\mathbf{x})p, \mathbf{v}), \quad \forall \mathbf{v} \in H_0(\text{div}; \Omega), \\ (c(\mathbf{x})p, q) + (\text{div}\mathbf{u}, q) &= (f, q), \quad \forall q \in L^2(\Omega). \end{aligned}$$

In the subsequence, we assume that there exist positive constants α_1, α_2 , and α_3 such that

$$(4) \quad \alpha_1 \leq c(\mathbf{x}) \leq \alpha_2,$$

and for any $\mathbf{v} \in (L^2(\Omega))^2$, $q \in L^2(\Omega)$

$$(5) \quad \alpha_3(\|q\|_{0,\Omega} + \|\mathbf{v}\|_{0,\Omega}) \leq (c(\mathbf{x})q, q) + (K^{-1}(\mathbf{x})\mathbf{v}, \mathbf{v}) - (\boldsymbol{\beta}(\mathbf{x})q, \mathbf{v}).$$

Under this assumption, it is well known that equations (1)-(3) have a unique solution for any given $f \in L^2(\Omega)$.

Let $\mathcal{T}_{h,i}$ be a conforming and regular triangulation of Ω_i , $1 \leq i \leq n$, allowing for the possibility that $\mathcal{T}_{h,i}$ and $\mathcal{T}_{h,j}$ need not match on $\Gamma_{i,j}$. $T_B \in \mathcal{T}_{h,i}$ stands for the triangle element in $\mathcal{T}_{h,i}$ whose barycenter is B . Let $\mathcal{T}_h = \cup_{i=1}^n \mathcal{T}_{h,i}$ be the union of all such block triangulations and E_i be the set of edges of $\mathcal{T}_{h,i}$. For any given edge $e \in E_i$, we denote two elements that share the common edge e by $T_{e,1}$ and $T_{e,2}$, and denote the midpoint of edge e by M_e . In particular, if the edge e is located on $\partial\Omega_i$, we regard $T_{e,2}$ as null set. Moreover, each partition $\mathcal{T}_{h,i}$, $1 \leq i \leq n$ would induce a partition of Γ_i , we denote it by $\Gamma_{h,i}$.

Next we construct the dual partition $\mathcal{T}_{h,i}^*$ associated with $\mathcal{T}_{h,i}$, $1 \leq i \leq n$. For any given edge $e \in E_i$, we define the dual element T_e^* that surrounds edge e as follows. As shown in Figure 1, the interior edge e is the common side of $T_{e,1} = \triangle A_1 A_2 A_3$ and

$T_{e,2} = \triangle A_1 A_3 A_4$, and B_1, B_2 are the barycenters of these two elements. Connect the nodes of $T_{e,1}$ and $T_{e,2}$ with the barycenters B_1, B_2 by straight segments. Thus, the quadrilateral $B_1 A_3 B_2 A_1$ (dashed quadrilateral in Figure 1.a) is defined as T_e^* . If edge e is located on $\partial\Omega_i$, the dual element T_e^* associated to e is a border triangular, see Figure 1.b. For the convenience, we further denote $T_{e,1} \cap T_e^*$ and $T_{e,2} \cap T_e^*$ by $T_{e,1}^*$ and $T_{e,2}^*$, respectively. Likewise, $T_{e,2}^*$ is regarded as a null set, if edge e is located on $\partial\Omega_i$.

On each $\mathcal{T}_{h,i}, 1 \leq i \leq n$, we take the lowest order Raviart-Thomas space $\mathbf{U}_{h,i}$ and the piecewise constant function space $W_{h,i}$ as trial function spaces to approximate the fluid velocity and the pressure, respectively. To be special,

$$\begin{aligned} \mathbf{U}_{h,i} &= \{ \mathbf{v}_{h,i} : \mathbf{v}_{h,i} |_{T} = (a + bx, c + by), a, b, c \in \mathbb{R}, \\ &\quad \forall T \in \mathcal{T}_{h,i}; \mathbf{v}_{h,i} \cdot \mathbf{n} = 0, \text{ on } \partial\Omega \}, \\ W_{h,i} &= \{ w_{h,i} : w_{h,i} |_{T} \text{ is a constant}, \forall T \in \mathcal{T}_{h,i} \}. \end{aligned}$$

Let

$$\begin{aligned} \mathbf{U}_h &= \{ \mathbf{v}_h : \mathbf{v}_h |_{\Omega_i} \in \mathbf{U}_{h,i}, i = 1, 2, \dots, n \}, \\ W_h &= \{ w_h : w_h |_{\Omega_i} \in W_{h,i}, i = 1, 2, \dots, n \}. \end{aligned}$$

The normal components of vectors in \mathbf{U}_h are continuous between elements within each block Ω_i , but there is no such restriction across Γ . Besides, define a operator $\gamma_h : \mathbf{U}_h \rightarrow (L^2(\Omega))^2$ as follows: for any $e \in E_i, i = 1, 2, \dots, n$,

$$(\gamma_h \mathbf{u}_h) |_{T_e^*} = \mathbf{u}_h |_{T_{e,1}} \chi_{T_{e,1}^*} + \mathbf{u}_h |_{T_{e,2}} \chi_{T_{e,2}^*},$$

where $\chi_{T_{e,1}^*}$ and $\chi_{T_{e,2}^*}$ are the characteristic functions of the sets $T_{e,1}^*$ and $T_{e,2}^*$, respectively. Thus, it is obvious that for a function $\mathbf{u}_h \in \mathbf{U}_h$ its projection $\gamma_h \mathbf{u}_h$ is a piecewise constant vector function, which can take different constant vector values on the left and right sides of an interior dual element and has continuous normal components between elements within each block Ω_i .

In order to ensure the continuity of p and flux on the non-matching interface $\Gamma_{i,j}$, we choose a parameter $\alpha > 0$ such that p and \mathbf{u} satisfy the following Robin type interface condition:

$$(6) \quad \alpha p_i - \mathbf{u}_i \cdot \mathbf{n}_i = \alpha p_j + \mathbf{u}_j \cdot \mathbf{n}_j \text{ on } \Gamma_{i,j}, i, j = 1, 2, \dots, n,$$

where \mathbf{u}_i is the trace of \mathbf{u} on $\partial\Omega_i$, and \mathbf{n}_i is the outward unit normal vector with respect to $\partial\Omega_i, 1 \leq i \leq n$. If the Robin type interface condition (6) is imposed twice on each interface $\Gamma_{k,l}$: once for $k = i, l = j$, once for $k = j, l = i$, we can have $p_i = p_j$ and $\mathbf{u}_i \cdot \mathbf{n}_i = -\mathbf{u}_j \cdot \mathbf{n}_j$, see [19].

Finally, on each $\Gamma_{h,i}, 1 \leq i \leq n$, we define a piecewise constant function space $\Lambda_{h,i}$, which is used to approximate the trace p_i in the discretization of (6). Similarly, let

$$(7) \quad \Lambda_h = \{ \lambda_h : \lambda_h |_{\Gamma_i} \in \Lambda_{h,i}, 1 \leq i \leq n \}.$$

3. MFV method on non-matching grids

Assume that the exact solution $p \in H^1(\Omega)$, then for any given $\mathbf{v}_h \in \mathcal{U}_h$ and $e \in E_i$, $1 \leq i \leq n$, we have

$$\begin{aligned}
\int_{T_e^*} -\nabla p \cdot \gamma_h \mathbf{v}_h d\mathbf{x} &= \int_{T_e^* \cap T_{e,1}} -\nabla p \cdot \gamma_h \mathbf{v}_h d\mathbf{x} + \int_{T_e^* \cap T_{e,2}} -\nabla p \cdot \gamma_h \mathbf{v}_h d\mathbf{x} \\
&= \int_{T_{e,1}^*} -\nabla p \cdot \gamma_h \mathbf{v}_h d\mathbf{x} + \int_{T_{e,2}^*} -\nabla p \cdot \gamma_h \mathbf{v}_h d\mathbf{x} \\
&= \int_{T_{e,1}^*} p \nabla \cdot (\gamma_h \mathbf{v}_h) d\mathbf{x} - \int_{\partial T_{e,1}^*} p(\gamma_h \mathbf{v}_h) \cdot \mathbf{n} ds \\
&\quad + \int_{T_{e,2}^*} p \nabla \cdot (\gamma_h \mathbf{v}_h) d\mathbf{x} - \int_{\partial T_{e,2}^*} p(\gamma_h \mathbf{v}_h) \cdot \mathbf{n} ds \\
(8) \quad &= - \int_{\partial T_{e,1}^*} p(\gamma_h \mathbf{v}_h) \cdot \mathbf{n} ds - \int_{\partial T_{e,2}^*} p(\gamma_h \mathbf{v}_h) \cdot \mathbf{n} ds,
\end{aligned}$$

where Green's formulation is used. If $e \in E_i$ is located in the interior of Ω_i , then p and the normal component of $\gamma_h \mathbf{v}_h$ are continuous across edge e , and if $e \in E_i$ is located on $\partial\Omega$, the normal component of $\gamma_h \mathbf{v}_h$ is zero. Therefore, summarising (8) over all edges $e \in E_i$ leads to

$$\begin{aligned}
(-\nabla p, \gamma_h \mathbf{v}_h)_i &= \sum_{e \in E_i} - \int_{\partial T_e^* \cap T_{e,1}} p \gamma_h \mathbf{v}_h |_{T_{e,1}} (M_e) \cdot \mathbf{n} ds \\
&\quad - \int_{\partial T_e^* \cap T_{e,2}} p \gamma_h \mathbf{v}_h |_{T_{e,2}} (M_e) \cdot \mathbf{n} ds - \langle p_i, \gamma_h \mathbf{v}_h \cdot \mathbf{n}_i \rangle_i.
\end{aligned}$$

Here and below, no matter if $e \in E_i$ is located on $\partial\Omega_i$, the notations $\partial T_e^* \cap T_{e,1}$ and $\partial T_e^* \cap T_{e,2}$ stand for the dual element edges which are located on the interiors of $T_{e,1}$ and $T_{e,2}$. For example, $\partial T_e^* \cap T_{e,1} = A_1 B_1 A_3$ and $\partial T_e^* \cap T_{e,2} = A_1 B_2 A_3$ in Figure 1.a, and $\partial T_e^* \cap T_{e,1} = A_1 B_1 A_3$ and $\partial T_e^* \cap T_{e,2} = \emptyset$ in Figure 1.b. Let

$$\begin{aligned}
B(p, \mathbf{v}_h)_i &= \sum_{e \in E_i} - \int_{\partial T_e^* \cap T_{e,1}} p \gamma_h \mathbf{v}_h |_{T_{e,1}} (M_e) \cdot \mathbf{n} ds \\
&\quad - \int_{\partial T_e^* \cap T_{e,2}} p \gamma_h \mathbf{v}_h |_{T_{e,2}} (M_e) \cdot \mathbf{n} ds, \\
B(p, \mathbf{v}_h) &= \sum_{i=1}^n B(p, \mathbf{v}_h)_i.
\end{aligned}$$

Using $\gamma_h \mathbf{v}_h$, $q_h \in W_h$, and $\mu_h \in \Lambda_h$ to test equations (1), (2), and (6), respectively, we obtain for $1 \leq i \leq n$,

$$(9) \quad (K^{-1}(\mathbf{x})\mathbf{u}, \gamma_h \mathbf{v}_h)_i = B(p, \mathbf{v}_h)_i + (\beta(\mathbf{x})p, \gamma_h \mathbf{v}_h)_i - \langle p_i, \gamma_h \mathbf{v}_h \cdot \mathbf{n}_i \rangle_i,$$

$$(10) \quad (c(\mathbf{x})p, q_h)_i + (\nabla \cdot \mathbf{u}, q_h)_i = (f, q_h)_i,$$

$$(11) \quad \langle \alpha p_i - \mathbf{u}_i \cdot \mathbf{n}_i, \mu_{h,i} \rangle_i = \sum_{j=1}^n \langle \alpha p_j + \mathbf{u}_j \cdot \mathbf{n}_j, \mu_{h,i} \rangle_{i,j},$$

where $\mu_{h,i} = \mu_h |_{\Gamma_i}$ for any $1 \leq i \leq n$.

Then, the MFV method we consider is: Find $\mathbf{u}_h \in \mathbf{U}_h, p_h \in W_h, \lambda_h \in \Lambda_h$ such that, for any $1 \leq i \leq n$,

$$(12) \quad \begin{aligned} & (K^{-1}(\mathbf{x})\mathbf{u}_h, \gamma_h \mathbf{v}_h)_i \\ & = B(p_h, \mathbf{v}_h)_i + (\boldsymbol{\beta}(\mathbf{x})p_h, \gamma_h \mathbf{v}_h)_i - \langle \lambda_{h,i}, \gamma_h \mathbf{v}_h \cdot \mathbf{n}_i \rangle_i, \forall \mathbf{v}_h \in \mathbf{U}_h, \end{aligned}$$

$$(13) \quad (c(\mathbf{x})p_h, q_h)_i + (\nabla \cdot \mathbf{u}_h, q_h)_i = (f, q_h)_i, \quad \forall q_h \in W_h,$$

$$(14) \quad \langle \alpha \lambda_{h,i} - \mathbf{u}_{h,i} \cdot \mathbf{n}_i, \mu_{h,i} \rangle_i = \sum_{j=1}^n \langle \alpha \lambda_{h,j} + \mathbf{u}_{h,j} \cdot \mathbf{n}_j, \mu_{h,i} \rangle_{i,j}, \quad \forall \mu_h \in \Lambda_h,$$

where for any $1 \leq i \leq n$, $\lambda_{h,i} = \lambda_h|_{\Gamma_i}$ and $\mathbf{u}_{h,i} = \mathbf{u}_h|_{\Omega_i}$.

Let $\|\cdot\|_i$ and $\|\cdot\|_{i,j}$ be the norms induced by the inner products $\langle \cdot, \cdot \rangle_i$ and $\langle \cdot, \cdot \rangle_{i,j}$ respectively. For any given $\mathbf{u}_h = (u_{1,h}, u_{2,h}) \in \mathbf{U}_h$, we define

$$\|\mathbf{u}_h\|_{1,h}^2 = \sum_{T \in \mathcal{T}_h} \|\nabla u_{1,h}\|_{0,T}^2 + \|\nabla u_{2,h}\|_{0,T}^2,$$

where $\|\cdot\|_{0,T}$ is the norm of $L^2(T)$. Moreover, we define

$$\tilde{H}^1(\Omega) = \{v : v|_{\Omega_i} \in H^1(\Omega_i), 1 \leq i \leq n\}.$$

There exists a projection $\Pi_{h,i}$ from $(H^1(\Omega_i))^2 \cap H_0(\text{div}; \Omega_i)$ onto $\mathbf{U}_{h,i}$, satisfying the following properties for any $\mathbf{q} \in (H^1(\Omega_i))^2 \cap H_0(\text{div}; \Omega_i)$, see [20],

$$(15) \quad (\nabla \cdot (\Pi_{h,i} \mathbf{q} - \mathbf{q}), w_{h,i})_i = 0, \quad \forall w_{h,i} \in W_{h,i},$$

$$(16) \quad \langle (\Pi_{h,i} \mathbf{q} - \mathbf{q}) \cdot \mathbf{n}_i, \mathbf{v}_{h,i} \cdot \mathbf{n}_i \rangle_i = 0, \quad \forall \mathbf{v}_{h,i} \in \mathbf{U}_{h,i}.$$

Furthermore, we define a projection Π_h from $(H^1(\Omega))^2 \cap H_0(\text{div}; \Omega)$ onto \mathbf{U}_h , satisfying

$$(17) \quad (\Pi_h \mathbf{q})|_{\Omega_i} = \Pi_{h,i}(\mathbf{q}|_{\Omega_i}), \quad \forall \mathbf{q} \in (H^1(\Omega))^2 \cap H_0(\text{div}; \Omega).$$

For any $g \in L^2(\Omega)$, let $\hat{g} \in W_h$ be its $L^2(\Omega)$ projection satisfying

$$(18) \quad (g - \hat{g}, w_h) = 0, \quad \forall w_h \in W_h.$$

Similarly, we define the projection of a function $g \in L^2(\Gamma_i)$ by $\bar{g} \in \Lambda_{h,i}$, satisfying

$$(19) \quad \langle g - \bar{g}, \mu_{h,i} \rangle_i = 0, \quad \forall \mu_{h,i} \in \Lambda_{h,i}.$$

In the rest of this article, h will denote the maximum grid size and the symbol C will denote a positive generic constant independent of h that may take on different values in different places.

In the theoretical analysis, the following lemmas are necessary.

Lemma 3.1. *For any $\mathbf{v}_h \in \mathbf{U}_h$ and $w_h \in W_h$, it follows that*

$$(20) \quad B(w_h, \mathbf{v}_h)_i = (\text{div} \mathbf{v}_h, w_h)_i.$$

Proof: First, $B(w_h, \mathbf{v}_h)_i$ can be rewritten as follows

$$\begin{aligned} B(w_h, \mathbf{v}_h)_i &= \sum_{e \in E_i} - \int_{\partial T_e^* \cap T_{e,1}} w_h \gamma_h \mathbf{v}_h|_{T_{e,1}} (M_e) \cdot \mathbf{n} ds \\ &\quad - \int_{\partial T_e^* \cap T_{e,2}} w_h \gamma_h \mathbf{v}_h|_{T_{e,2}} (M_e) \cdot \mathbf{n} ds, \\ &= \sum_{T \in \mathcal{T}_{h,i}} Q_T(w_h, \mathbf{v}_h), \end{aligned}$$

where

$$(21) \quad Q_T(w_h, \mathbf{v}_h) = \sum_{e \in \partial T} - \int_{\partial T_e^* \cap T} w_h \gamma_h \mathbf{v}_h |_T (M_e) \cdot \mathbf{n} ds.$$

Here, the notation $\partial T_e^* \cap T$ still does not include the edge e , when e is located on $\partial \Omega_i$. For example, $\partial T_e^* \cap T = A_1 B_1 A_3$ in Figure 1.b. From the definition of operator γ_h , we have

$$Q_T(w_h, \mathbf{v}_h) = \sum_{e \in \partial T} - \int_{\partial T_e^* \cap T} w_h \mathbf{v}_h |_T (M_e) \cdot \mathbf{n} ds.$$

Moreover, using Green's formula yields

$$(22) \quad \begin{aligned} Q_T(w_h, \mathbf{v}_h) &= \sum_{e \in \partial T} \int_e w_h \mathbf{v}_h |_T (M_e) \cdot \mathbf{n} ds - \int_{T_e^* \cap T} w_h \operatorname{div}(\mathbf{v}_h |_T (M_e)) dx \\ &= \sum_{e \in \partial T} \int_e w_h \mathbf{v}_h |_T (M_e) \cdot \mathbf{n} ds. \end{aligned}$$

On each element $T \in \mathcal{T}_{h,i}$, w_h is a constant, and each component of \mathbf{v}_h is a linear polynomial. In addition, M_e is the midpoint of edge e . Therefore, we have from (22) that

$$(23) \quad Q_T(w_h, \mathbf{v}_h) = \sum_{e \in \partial T} \int_e w_h \mathbf{v}_h |_T \cdot \mathbf{n} ds.$$

Again, it follows from Green's formula that

$$(24) \quad \begin{aligned} Q_T(w_h, \mathbf{v}_h) &= \int_T w_h \operatorname{div} \mathbf{v}_h dx + \int_T \nabla w_h \cdot \mathbf{v}_h dx \\ &= \int_T w_h \operatorname{div} \mathbf{v}_h dx. \end{aligned}$$

Thus, we get the desired result by summing (24) over $T \in \mathcal{T}_{h,i}$. \square

Lemma 3.2. *For any $\mathbf{v}_h \in \mathbf{U}_h$, there holds that*

$$(25) \quad \|\mathbf{v}_h - \gamma_h \mathbf{v}_h\|_{0,\Omega} \leq Ch |\mathbf{v}_h|_{1,h}.$$

Proof: Let $\mathbf{v}_h = (v_{1,h}, v_{2,h}) \in \mathbf{U}_h$. First, we have

$$(26) \quad \|\mathbf{v}_h - \gamma_h \mathbf{v}_h\|_{0,\Omega}^2 = \sum_{T \in \mathcal{T}_h} \|\mathbf{v}_h - \gamma_h \mathbf{v}_h\|_{0,T}^2.$$

On each element $T \in \mathcal{T}_h$, if \mathbf{v}_h is a constant vector, then $\mathbf{v}_h - \gamma_h \mathbf{v}_h = 0$. Therefore, by Theorem 5 with scaling in [12], we get

$$(27) \quad \|\mathbf{v}_h - \gamma_h \mathbf{v}_h\|_{0,T}^2 \leq Ch^2 (|v_{1,h}|_{1,T}^2 + |v_{2,h}|_{1,T}^2).$$

Combining (26) and (27) leads to

$$\|\mathbf{v}_h - \gamma_h \mathbf{v}_h\|_{0,\Omega} \leq Ch |\mathbf{v}_h|_{1,h}.$$

\square

4. Solvability and Convergence

In the following theorem, we present that the proposed MFV method (12)-(14) has a unique solution.

Theorem 4.1. *If the coefficients of system (1)-(3) satisfy the assumptions (4) and (5) and h is sufficiently small, then there exists a unique solution to the MFV method (12)-(14).*

Proof: In (12) and (13), take the test functions $\mathbf{v}_h = \mathbf{u}_h$ and $q_h = p_h$, plus them, cancel the terms $B(p_h, \mathbf{u}_h)_i$ and $(\operatorname{div} \mathbf{u}_h, p_h)_i$, and sum over i to get

$$(c(\mathbf{x})p_h, p_h) + (K^{-1}(\mathbf{x})\mathbf{u}_h, \gamma_h \mathbf{u}_h) = (\boldsymbol{\beta}(\mathbf{x})p_h, \gamma_h \mathbf{u}_h) - \sum_{i=1}^n \langle \lambda_{h,i}, \gamma_h \mathbf{u}_h \cdot \mathbf{n}_i \rangle_i + (f, p_h).$$

Compared with the non-mortar mixed finite element method proposed in [19], there is not any change in the third equation (14). Therefore, we employ the same way to estimate (14). First, the following two equalities are valid, refer to [19] for more details.

$$\begin{aligned} \frac{1}{4}\alpha \sum_{i,j=1}^n \langle \lambda_{h,i} - \lambda_{h,j}, \lambda_{h,i} - \lambda_{h,j} \rangle_{i,j} &= \frac{1}{2} \sum_{i,j=1}^n \langle \mathbf{u}_{h,i} \cdot \mathbf{n}_i + \mathbf{u}_{h,j} \cdot \mathbf{n}_j, \lambda_{h,i} \rangle_{i,j}, \\ \frac{1}{4\alpha} \sum_{i,j=1}^n \langle \mathbf{u}_{h,i} \cdot \mathbf{n}_i + \mathbf{u}_{h,j} \cdot \mathbf{n}_j, \mathbf{u}_{h,i} \cdot \mathbf{n}_i + \mathbf{u}_{h,j} \cdot \mathbf{n}_j \rangle_{i,j} \\ &= \frac{1}{2} \sum_{i,j=1}^n \langle \lambda_{h,i}, \mathbf{u}_{h,i} \cdot \mathbf{n}_i - \mathbf{u}_{h,j} \cdot \mathbf{n}_j \rangle_{i,j}. \end{aligned}$$

Next, summing the above three equalities yields

$$\begin{aligned} (28) \quad &(c(\mathbf{x})p_h, p_h) + (K^{-1}(\mathbf{x})\mathbf{u}_h, \gamma_h \mathbf{u}_h) + \frac{1}{4}\alpha \sum_{i,j=1}^n \langle \lambda_{h,i} - \lambda_{h,j}, \lambda_{h,i} - \lambda_{h,j} \rangle_{i,j} \\ &+ \frac{1}{4\alpha} \sum_{i,j=1}^n \langle \mathbf{u}_{h,i} \cdot \mathbf{n}_i + \mathbf{u}_{h,j} \cdot \mathbf{n}_j, \mathbf{u}_{h,i} \cdot \mathbf{n}_i + \mathbf{u}_{h,j} \cdot \mathbf{n}_j \rangle_{i,j} \\ &= (\boldsymbol{\beta}(\mathbf{x})p_h, \gamma_h \mathbf{u}_h) + \sum_{i=1}^n \langle \lambda_{h,i}, (\mathbf{u}_h - \gamma_h \mathbf{u}_h) \cdot \mathbf{n}_i \rangle_i + (f, p_h). \end{aligned}$$

In equation (28) we set $f = 0$, and rewrite it as follows

$$\begin{aligned} &(c(\mathbf{x})p_h, p_h) + (K^{-1}(\mathbf{x})\mathbf{u}_h, \mathbf{u}_h) - (\boldsymbol{\beta}(\mathbf{x})p_h, \mathbf{u}_h) \\ &+ \frac{1}{4}\alpha \sum_{i,j=1}^n \langle \lambda_{h,i} - \lambda_{h,j}, \lambda_{h,i} - \lambda_{h,j} \rangle_{i,j} \\ &+ \frac{1}{4\alpha} \sum_{i,j=1}^n \langle \mathbf{u}_{h,i} \cdot \mathbf{n}_i + \mathbf{u}_{h,j} \cdot \mathbf{n}_j, \mathbf{u}_{h,i} \cdot \mathbf{n}_i + \mathbf{u}_{h,j} \cdot \mathbf{n}_j \rangle_{i,j} \\ &= (K^{-1}(\mathbf{x})\mathbf{u}_h, (\mathbf{u}_h - \gamma_h \mathbf{u}_h)) + (\boldsymbol{\beta}(\mathbf{x})p_h, \gamma_h \mathbf{u}_h - \mathbf{u}_h) \\ &+ \sum_{i=1}^n \langle \lambda_{h,i}, (\mathbf{u}_h - \gamma_h \mathbf{u}_h) \cdot \mathbf{n}_i \rangle_i. \end{aligned}$$

By the assumption (5), we have

$$\begin{aligned}
(29) \quad & C(\|p_h\|_{0,\Omega}^2 + \|\mathbf{u}_h\|_{0,\Omega}^2) + \frac{1}{4}\alpha \sum_{i,j=1}^n \|\lambda_{h,i} - \lambda_{h,j}\|_{i,j}^2 \\
& + \frac{1}{4\alpha} \sum_{i,j=1}^n \|\mathbf{u}_{h,i} \cdot \mathbf{n}_i + \mathbf{u}_{h,j} \cdot \mathbf{n}_j\|_{i,j}^2 \\
& \leq (K^{-1}(\mathbf{x})\mathbf{u}_h, (\mathbf{u}_h - \gamma_h \mathbf{u}_h)) + (\beta(\mathbf{x})p_h, \gamma_h \mathbf{u}_h - \mathbf{u}_h) \\
& + \sum_{i=1}^n \langle \lambda_{h,i}, (\mathbf{u}_h - \gamma_h \mathbf{u}_h) \cdot \mathbf{n}_i \rangle_i.
\end{aligned}$$

Now we begin to estimate the three terms on the right hand side of (29). For the first term, we have

$$\begin{aligned}
(30) \quad & |(K^{-1}(\mathbf{x})\mathbf{u}_h, (\mathbf{u}_h - \gamma_h \mathbf{u}_h))| \leq C \|\mathbf{u}_h\|_{0,\Omega} \|\mathbf{u}_h - \gamma_h \mathbf{u}_h\|_{0,\Omega} \\
& \leq Ch \|\mathbf{u}_h\|_{0,\Omega} |\mathbf{u}_h|_{1,h},
\end{aligned}$$

where Lemma 3.2 is used. Similarly, the second term satisfies that

$$\begin{aligned}
(31) \quad & |(\beta(\mathbf{x})p_h, \gamma_h \mathbf{u}_h - \mathbf{u}_h)| \leq C \|p_h\|_{0,\Omega} \|\mathbf{u}_h - \gamma_h \mathbf{u}_h\|_{0,\Omega} \\
& \leq Ch \|p_h\|_{0,\Omega} |\mathbf{u}_h|_{1,h}.
\end{aligned}$$

For the third term, because $\lambda_{h,i}$ is a piecewise constant function on the partition $\Gamma_{h,i}$, we have

$$\sum_{i=1}^n \langle \lambda_{h,i}, (\mathbf{u}_h - \gamma_h \mathbf{u}_h) \cdot \mathbf{n}_i \rangle_i = \sum_{i=1}^n \sum_{e \in \Gamma_{h,i}} \lambda_{h,i} \int_e (\mathbf{u}_h - \gamma_h \mathbf{u}_h) \cdot \mathbf{n}_i ds,$$

where the element e in $\Gamma_{h,i}$ is also an edge in the triangulation $\mathcal{T}_{h,i}$. By the definition of $\gamma_h \mathbf{u}_h$, we have

$$\begin{aligned}
(32) \quad & \sum_{i=1}^n \langle \lambda_{h,i}, (\mathbf{u}_h - \gamma_h \mathbf{u}_h) \cdot \mathbf{n}_i \rangle_i = \sum_{i=1}^n \sum_{e \in \Gamma_{h,i}} \lambda_{h,i} \int_e (\mathbf{u}_h - \mathbf{u}_h(M_e)) \cdot \mathbf{n}_i ds \\
& = 0,
\end{aligned}$$

where M_e is the midpoint of e .

In equation (13), taking $q_h = \operatorname{div} \mathbf{u}_h$ and $f = 0$ yields

$$\|\operatorname{div} \mathbf{u}_h\|_{0,\Omega}^2 = -(c(\mathbf{x})p_h, \operatorname{div} \mathbf{u}_h),$$

By the assumption (4), we have

$$\|\operatorname{div} \mathbf{u}_h\|_{0,\Omega}^2 \leq C \|p_h\|_{0,\Omega} \|\operatorname{div} \mathbf{u}_h\|_{0,\Omega}.$$

This implies that

$$\|\operatorname{div} \mathbf{u}_h\|_{0,\Omega} \leq C \|p_h\|_{0,\Omega}.$$

Since $|\mathbf{u}_h|_{1,h} \leq C \|\operatorname{div} \mathbf{u}_h\|_{0,\Omega}$, we get

$$|\mathbf{u}_h|_{1,h} \leq C \|p_h\|_{0,\Omega}.$$

Thus, the inequalities (30) and (31) can be further estimated as

$$(33) \quad |(K^{-1}(\mathbf{x})\mathbf{u}_h, (\mathbf{u}_h - \gamma_h \mathbf{u}_h))| \leq C(h \|\mathbf{u}_h\|_{0,\Omega}^2 + h \|p_h\|_{0,\Omega}^2),$$

$$(34) \quad |(\beta(\mathbf{x})p_h, \gamma_h \mathbf{u}_h - \mathbf{u}_h)| \leq Ch \|p_h\|_{0,\Omega}^2,$$

where inequality (33) is obtained by using the usual Cauchy-Schwarz inequality.

Finally, combining (29), (32), (33) and (34), we have

$$\begin{aligned} & C(1-h) \|p_h\|_{0,\Omega}^2 + C(1-h) \|\mathbf{u}_h\|_{0,\Omega}^2 + \frac{1}{4}\alpha \sum_{i,j=1}^n \|\lambda_{h,i} - \lambda_{h,j}\|_{i,j}^2 \\ & + \frac{1}{4\alpha} \sum_{i,j=1}^n \|\mathbf{u}_{h,i} \cdot \mathbf{n}_i + \mathbf{u}_{h,j} \cdot \mathbf{n}_j\|_{i,j}^2 \leq 0. \end{aligned}$$

It is obvious that $p_h = 0$ and $\mathbf{u}_h = 0$, provided sufficiently small h . Then (12) implies that $\lambda_{h,i} = 0, 1 \leq i \leq n$. Thus, the proof of Theorem 4.1 is completed. \square

Now, we show the convergence result in the following theorem for our MFV method (12)-(14).

Theorem 4.2. *Let $\mathcal{T}_{h,i}$ be a regular triangulation, $\{\mathbf{u}_h, p_h, \lambda_h\}$ be the solution of the problem (12)-(14), and $\{\mathbf{u}, p\}$ be the solution of the problem (1)-(3). Under the assumptions (4) and (5), then there holds that*

$$\begin{aligned} (35) \quad & \|p - p_h\|_{0,\Omega} + \|\mathbf{u} - \mathbf{u}_h\|_{0,\Omega} + (\alpha \sum_{i,j=1}^n \|\lambda_{h,i} - \lambda_{h,j}\|_{i,j}^2)^{1/2} \\ & + (\frac{1}{\alpha} \sum_{i,j=1}^n \|\mathbf{u}_{h,i} \cdot \mathbf{n}_i + \mathbf{u}_{h,j} \cdot \mathbf{n}_j\|_{i,j}^2)^{1/2} \\ & \leq Ch \{ \|p\|_{1,\Omega} + (\sum_{i=1}^n \|\mathbf{u}\|_{1,\Omega_i}^2)^{1/2} + (\sum_{i=1}^n \alpha \|p_i\|_{1,\Gamma_i}^2)^{1/2} \\ & + (\sum_{i=1}^n \frac{1}{\alpha} \|\mathbf{u}_i\|_{1,\Gamma_i}^2)^{1/2} \}, \end{aligned}$$

provided that $\mathbf{u} \in H_0(\text{div}, \Omega) \cap (\tilde{H}^1(\Omega))^2$, $p \in H^1(\Omega)$, and the traces $\mathbf{u}_i \in (H^1(\Gamma_i))^2$, $p_i \in H^1(\Gamma_i)$.

Proof: For the convenience of analysis, we define the errors as

$$\varphi = p - p_h, \quad \boldsymbol{\psi} = \mathbf{u} - \mathbf{u}_h, \quad \phi_i = p_i - \lambda_{h,i}.$$

Subtract (12) and (13) from (9) and (10), respectively, and sum over i to obtain

$$(36) \quad (K^{-1}(\mathbf{x})\boldsymbol{\psi}, \gamma_h \mathbf{v}_h) = B(\varphi, \mathbf{v}_h) + (\boldsymbol{\beta}(\mathbf{x})\varphi, \gamma_h \mathbf{v}_h) - \sum_{i=1}^n \langle \phi_i, \gamma_h \mathbf{v}_h \cdot \mathbf{n}_i \rangle_i, \quad \forall \mathbf{v}_h \in \mathbf{U}_h,$$

$$(37) \quad (c(\mathbf{x})\varphi, q_h) + (\text{div} \boldsymbol{\psi}, q_h) = 0, \quad \forall q_h \in W_h.$$

Taking $\mathbf{v}_h = \Pi_h \boldsymbol{\psi}$ and $q_h = \hat{\varphi}$ in (36) and (37), respectively, and then summing these two equations leads to

$$\begin{aligned} (38) \quad & (c(\mathbf{x})\varphi, \hat{\varphi}) + (K^{-1}(\mathbf{x})\boldsymbol{\psi}, \gamma_h(\Pi_h \boldsymbol{\psi})) + (\text{div} \boldsymbol{\psi}, \hat{\varphi}) = B(\varphi, \Pi_h \boldsymbol{\psi}) + (\boldsymbol{\beta}(\mathbf{x})\varphi, \gamma_h(\Pi_h \boldsymbol{\psi})) \\ & - \sum_{i=1}^n \langle \phi_i, \gamma_h(\Pi_h \boldsymbol{\psi}) \cdot \mathbf{n}_i \rangle_i. \end{aligned}$$

The first two terms of the left hand side of (38) can be formulated as

$$(39) \quad (c(\mathbf{x})\varphi, \hat{\varphi}) = (c(\mathbf{x})\varphi, \varphi) + (c(\mathbf{x})\varphi, \hat{\varphi} - \varphi),$$

$$(40) \quad (K^{-1}(\mathbf{x})\boldsymbol{\psi}, \gamma_h(\Pi_h \boldsymbol{\psi})) = (K^{-1}(\mathbf{x})\boldsymbol{\psi}, \boldsymbol{\psi}) + (K^{-1}(\mathbf{x})\boldsymbol{\psi}, \gamma_h(\Pi_h \boldsymbol{\psi}) - \Pi_h \boldsymbol{\psi}) \\ + (K^{-1}(\mathbf{x})\boldsymbol{\psi}, \Pi_h \boldsymbol{\psi} - \boldsymbol{\psi}).$$

Due to

$$\begin{aligned}\widehat{\varphi} - \varphi &= (\widehat{p} - p_h) - (p - p_h) = \widehat{p} - p, \\ \Pi_h \boldsymbol{\psi} - \boldsymbol{\psi} &= (\Pi_h \mathbf{u} - \mathbf{u}_h) - (\mathbf{u} - \mathbf{u}_h) = \Pi_h \mathbf{u} - \mathbf{u},\end{aligned}$$

we further have

$$(41) \quad (c(\mathbf{x})\varphi, \widehat{\varphi}) = (c(\mathbf{x})\varphi, \varphi) + (c(\mathbf{x})\varphi, \widehat{p} - p),$$

$$(42) \quad (K^{-1}(\mathbf{x})\boldsymbol{\psi}, \gamma_h(\Pi_h \boldsymbol{\psi})) = (K^{-1}(\mathbf{x})\boldsymbol{\psi}, \boldsymbol{\psi}) + (K^{-1}(\mathbf{x})\boldsymbol{\psi}, \gamma_h(\Pi_h \boldsymbol{\psi}) - \Pi_h \boldsymbol{\psi}) \\ + (K^{-1}(\mathbf{x})\boldsymbol{\psi}, \Pi_h \mathbf{u} - \mathbf{u}).$$

Similarly, the last two terms of the right hand side of (38) can be formulated as

$$(43) \quad (\boldsymbol{\beta}(\mathbf{x})\varphi, \gamma_h(\Pi_h \boldsymbol{\psi})) = (\boldsymbol{\beta}(\mathbf{x})\varphi, \boldsymbol{\psi}) + (\boldsymbol{\beta}(\mathbf{x})\varphi, \gamma_h(\Pi_h \boldsymbol{\psi}) - \Pi_h \boldsymbol{\psi}) \\ + (\boldsymbol{\beta}(\mathbf{x})\varphi, \Pi_h \mathbf{u} - \mathbf{u}),$$

$$(44) \quad - \sum_{i=1}^n \langle \phi_i, \gamma_h(\Pi_h \boldsymbol{\psi}) \cdot \mathbf{n}_i \rangle_i = \sum_{i=1}^n \langle \phi_i, (\Pi_h \boldsymbol{\psi} - \gamma_h(\Pi_h \boldsymbol{\psi})) \cdot \mathbf{n}_i \rangle_i \\ - \sum_{i=1}^n \langle \phi_i, \Pi_h \boldsymbol{\psi} \cdot \mathbf{n}_i \rangle_i.$$

Now turn to consider the terms $(\operatorname{div} \boldsymbol{\psi}, \widehat{\varphi})$ and $B(\varphi, \Pi_h \boldsymbol{\psi})$ in (38). It follows from the definitions of Π_h and $\widehat{\varphi}$ that

$$(\operatorname{div} \boldsymbol{\psi}, \widehat{\varphi}) = (\operatorname{div}(\Pi_h \boldsymbol{\psi}), \widehat{\varphi}) = (\operatorname{div}(\Pi_h \boldsymbol{\psi}), \varphi).$$

Using Green's formula in above equation yields

$$(45) \quad (\operatorname{div} \boldsymbol{\psi}, \widehat{\varphi}) = \sum_{T \in \mathcal{T}_h} \sum_{e \in \partial T} \int_e (\Pi_h \boldsymbol{\psi}) \cdot \mathbf{n} \varphi ds - (\Pi_h \boldsymbol{\psi}, \nabla \varphi).$$

Besides,

$$(46) \quad \begin{aligned} B(\varphi, \Pi_h \boldsymbol{\psi}) &= \sum_{i=1}^n B(\varphi, \Pi_h \boldsymbol{\psi})_i \\ &= \sum_{i=1}^n \sum_{e \in E_i} \left\{ - \int_{\partial T_e^* \cap T_{e,1}} \varphi \gamma_h(\Pi_h \boldsymbol{\psi})|_{T_{e,1}}(M_e) \cdot \mathbf{n} ds \right. \\ &\quad \left. - \int_{\partial T_e^* \cap T_{e,2}} \varphi \gamma_h(\Pi_h \boldsymbol{\psi})|_{T_{e,2}}(M_e) \cdot \mathbf{n} ds \right\} \\ &= \sum_{T \in \mathcal{T}_h} \sum_{e \in \partial T} - \int_{\partial T_e^* \cap T} \varphi \gamma_h(\Pi_h \boldsymbol{\psi})|_T(M_e) \cdot \mathbf{n} ds. \end{aligned}$$

Here, the notation $\partial T_e^* \cap T$ has the same meaning as that in (21). Again using Green's formula in (46), we have

$$(47) \quad B(\varphi, \Pi_h \boldsymbol{\psi}) = \sum_{T \in \mathcal{T}_h} \sum_{e \in \partial T} \int_e \varphi \gamma_h(\Pi_h \boldsymbol{\psi})|_T(M_e) \cdot \mathbf{n} ds - (\gamma_h(\Pi_h \boldsymbol{\psi}), \nabla \varphi).$$

Thus, subtracting (45) from (47) leads to

$$\begin{aligned}
 (48) \quad B(\varphi, \Pi_h \boldsymbol{\psi}) - (\operatorname{div} \boldsymbol{\psi}, \widehat{\varphi}) &= \sum_{T \in \mathcal{T}_h} \sum_{e \in \partial T} \int_e \varphi(\gamma_h(\Pi_h \boldsymbol{\psi})|_T(M_e) \\
 &\quad - \Pi_h \boldsymbol{\psi}) \cdot \mathbf{n} ds - (\gamma_h(\Pi_h \boldsymbol{\psi}) - \Pi_h \boldsymbol{\psi}, \nabla \varphi) \\
 &= \sum_{T \in \mathcal{T}_h} \sum_{e \in \partial T} \int_e (p - p_h)((\Pi_h \boldsymbol{\psi})|_T(M_e) \\
 &\quad - \Pi_h \boldsymbol{\psi}) \cdot \mathbf{n} ds - (\gamma_h(\Pi_h \boldsymbol{\psi}) - \Pi_h \boldsymbol{\psi}, \nabla \varphi).
 \end{aligned}$$

Similar to (22) and (23), the following equality holds

$$(49) \quad \sum_{T \in \mathcal{T}_h} \sum_{e \in \partial T} \int_e p_h((\Pi_h \boldsymbol{\psi})|_T(M_e) - \Pi_h \boldsymbol{\psi}) \cdot \mathbf{n} ds = 0.$$

Since p and the normal component of $\Pi_h \boldsymbol{\psi}$ are continuous within each block, we have

$$\begin{aligned}
 (50) \quad &\sum_{T \in \mathcal{T}_h} \sum_{e \in \partial T} \int_e p((\Pi_h \boldsymbol{\psi})|_T(M_e) - \Pi_h \boldsymbol{\psi}) \cdot \mathbf{n} ds \\
 &= \sum_{i=1}^n \sum_{e \in \Gamma_{h,i}} \int_e p((\Pi_h \boldsymbol{\psi})(M_e) - \Pi_h \boldsymbol{\psi}) \cdot \mathbf{n} ds.
 \end{aligned}$$

Because \bar{p}_i is a constant on $e \in \Gamma_{h,i}$, one can get

$$\int_e \bar{p}_i((\Pi_h \boldsymbol{\psi})(M_e) - \Pi_h \boldsymbol{\psi}) \cdot \mathbf{n} ds = 0.$$

Then it holds that

$$\begin{aligned}
 (51) \quad &\sum_{T \in \mathcal{T}_h} \sum_{e \in \partial T} \int_e p((\Pi_h \boldsymbol{\psi})|_T(M_e) - \Pi_h \boldsymbol{\psi}) \cdot \mathbf{n} ds \\
 &= \sum_{i=1}^n \sum_{e \in \Gamma_{h,i}} \int_e (p - \bar{p}_i)((\Pi_h \boldsymbol{\psi})(M_e) - \Pi_h \boldsymbol{\psi}) \cdot \mathbf{n} ds.
 \end{aligned}$$

Combining (48), (49) and (51) yields

$$\begin{aligned}
 (52) \quad B(\varphi, \Pi_h \boldsymbol{\psi}) - (\operatorname{div} \boldsymbol{\psi}, \widehat{\varphi}) &= \sum_{i=1}^n \sum_{e \in \Gamma_{h,i}} \int_e (p - \bar{p}_i)((\Pi_h \boldsymbol{\psi})(M_e) - \Pi_h \boldsymbol{\psi}) \cdot \mathbf{n} ds \\
 &\quad - (\gamma_h(\Pi_h \boldsymbol{\psi}) - \Pi_h \boldsymbol{\psi}, \nabla \varphi) \\
 &= \sum_{i=1}^n \langle p - \bar{p}_i, (\gamma_h(\Pi_h \boldsymbol{\psi}) - \Pi_h \boldsymbol{\psi}) \cdot \mathbf{n}_i \rangle_i \\
 &\quad - (\gamma_h(\Pi_h \boldsymbol{\psi}) - \Pi_h \boldsymbol{\psi}, \nabla \varphi).
 \end{aligned}$$

Substitute (41), (42), (43), (44) and (52) into (38) to obtain

$$\begin{aligned}
(53) \quad & (c(\mathbf{x})\varphi, \varphi) + (K^{-1}(\mathbf{x})\boldsymbol{\psi}, \boldsymbol{\psi}) - (\boldsymbol{\beta}(\mathbf{x})\varphi, \boldsymbol{\psi}) \\
& = (c(\mathbf{x})\varphi, p - \widehat{p}) + (K^{-1}(\mathbf{x})\boldsymbol{\psi}, \mathbf{u} - \Pi_h \mathbf{u}) - (\boldsymbol{\beta}(\mathbf{x})\varphi, \mathbf{u} - \Pi_h \mathbf{u}) \\
& \quad + (K^{-1}(\mathbf{x})\boldsymbol{\psi}, \Pi_h \boldsymbol{\psi} - \gamma_h(\Pi_h \boldsymbol{\psi})) + (\boldsymbol{\beta}(\mathbf{x})\varphi, \gamma_h(\Pi_h \boldsymbol{\psi}) - \Pi_h \boldsymbol{\psi}) \\
& \quad + \sum_{i=1}^n \langle \phi_i, (\Pi_h \boldsymbol{\psi} - \gamma_h(\Pi_h \boldsymbol{\psi})) \cdot \mathbf{n}_i \rangle_i - \sum_{i=1}^n \langle \phi_i, \Pi_h \boldsymbol{\psi} \cdot \mathbf{n}_i \rangle_i \\
& \quad + \sum_{i=1}^n \langle p - \bar{p}_i, (\gamma_h(\Pi_h \boldsymbol{\psi}) - \Pi_h \boldsymbol{\psi}) \cdot \mathbf{n}_i \rangle_i - (\gamma_h(\Pi_h \boldsymbol{\psi}) - \Pi_h \boldsymbol{\psi}, \nabla \varphi).
\end{aligned}$$

Since the equations (14) and (11) are the same as the MFE method in [19], the authors of [19] have derived

$$\begin{aligned}
(54) \quad & \sum_{i,j=1}^n \alpha \|\phi_i - \phi_j\|_{i,j}^2 + \sum_{i,j=1}^n \frac{1}{\alpha} \|\boldsymbol{\psi}_i \cdot \mathbf{n}_i + \boldsymbol{\psi}_j \cdot \mathbf{n}_j\|_{i,j}^2 \\
& \leq C(\alpha \|p - \bar{p}_i\|_i^2 + \frac{1}{\alpha} \|(\mathbf{u} - \Pi_h \mathbf{u}) \cdot \mathbf{n}_i\|_i^2) + \sum_{i=1}^n \langle \phi_i, \Pi_h \boldsymbol{\psi} \cdot \mathbf{n}_i \rangle_i.
\end{aligned}$$

Taking $q_h = \operatorname{div} \Pi_h \boldsymbol{\psi}$ in (37), we have

$$(55) \quad - (c(\mathbf{x})\varphi, \operatorname{div} \Pi_h \boldsymbol{\psi}) = (\operatorname{div} \boldsymbol{\psi}, \operatorname{div} \Pi_h \boldsymbol{\psi}) = (\operatorname{div} \Pi_h \boldsymbol{\psi}, \operatorname{div} \Pi_h \boldsymbol{\psi}),$$

where the second equality is derived by using (15). Thus, it follows from (55) that

$$(56) \quad \|\Pi_h \boldsymbol{\psi}\|_{1,h} \leq C \|\operatorname{div} \Pi_h \boldsymbol{\psi}\|_{0,\Omega} \leq C \|\varphi\|_{0,\Omega}.$$

Now, we begin to estimate equation (53). First, from the assumption (5), we have

$$\begin{aligned}
(57) \quad & C(\|\varphi\|_{0,\Omega}^2 + \|\boldsymbol{\psi}\|_{0,\Omega}^2) \\
& \leq (c(\mathbf{x})\varphi, p - \widehat{p}) + (K^{-1}(\mathbf{x})\boldsymbol{\psi}, \mathbf{u} - \Pi_h \mathbf{u}) - (\boldsymbol{\beta}(\mathbf{x})\varphi, \mathbf{u} - \Pi_h \mathbf{u}) \\
& \quad + (K^{-1}(\mathbf{x})\boldsymbol{\psi}, \Pi_h \boldsymbol{\psi} - \gamma_h(\Pi_h \boldsymbol{\psi})) + (\boldsymbol{\beta}(\mathbf{x})\varphi, \gamma_h(\Pi_h \boldsymbol{\psi}) - \Pi_h \boldsymbol{\psi}) \\
& \quad + \sum_{i=1}^n \langle \phi_i, (\Pi_h \boldsymbol{\psi} - \gamma_h(\Pi_h \boldsymbol{\psi})) \cdot \mathbf{n}_i \rangle_i - \sum_{i=1}^n \langle \phi_i, \Pi_h \boldsymbol{\psi} \cdot \mathbf{n}_i \rangle_i \\
& \quad + \sum_{i=1}^n \langle p - \bar{p}_i, (\gamma_h(\Pi_h \boldsymbol{\psi}) - \Pi_h \boldsymbol{\psi}) \cdot \mathbf{n}_i \rangle_i - (\gamma_h(\Pi_h \boldsymbol{\psi}) - \Pi_h \boldsymbol{\psi}, \nabla \varphi).
\end{aligned}$$

From the Young's inequality, we know that the first three terms of the right hand side of (57) satisfy

$$\begin{aligned}
(58) \quad & |(c(\mathbf{x})\varphi, p - \widehat{p})| \leq C \|\varphi\|_{0,\Omega} \|p - \widehat{p}\|_{0,\Omega} \\
& \leq C\varepsilon \|\varphi\|_{0,\Omega}^2 + \frac{C}{\varepsilon} \|p - \widehat{p}\|_{0,\Omega}^2,
\end{aligned}$$

$$\begin{aligned}
(59) \quad & |(K^{-1}(\mathbf{x})\boldsymbol{\psi}, \mathbf{u} - \Pi_h \mathbf{u})| \leq C \|\boldsymbol{\psi}\|_{0,\Omega} \|\mathbf{u} - \Pi_h \mathbf{u}\|_{0,\Omega} \\
& \leq C\varepsilon \|\boldsymbol{\psi}\|_{0,\Omega}^2 + \frac{C}{\varepsilon} \|\mathbf{u} - \Pi_h \mathbf{u}\|_{0,\Omega}^2,
\end{aligned}$$

$$\begin{aligned}
(60) \quad & |-(\boldsymbol{\beta}(\mathbf{x})\varphi, \mathbf{u} - \Pi_h \mathbf{u})| \leq C \|\varphi\|_{0,\Omega} \|\mathbf{u} - \Pi_h \mathbf{u}\|_{0,\Omega} \\
& \leq C\varepsilon \|\varphi\|_{0,\Omega}^2 + \frac{C}{\varepsilon} \|\mathbf{u} - \Pi_h \mathbf{u}\|_{0,\Omega}^2,
\end{aligned}$$

where ε is a positive constant, which will be determined at the end of this proof. It follows from (25) and (56) that

$$\begin{aligned}
& (K^{-1}(\mathbf{x})\boldsymbol{\psi}, \Pi_h \boldsymbol{\psi} - \gamma_h(\Pi_h \boldsymbol{\psi})) + (\boldsymbol{\beta}(\mathbf{x})\varphi, \gamma_h(\Pi_h \boldsymbol{\psi}) - \Pi_h \boldsymbol{\psi}) \\
& \leq C \|\boldsymbol{\psi}\|_{0,\Omega} \|\Pi_h \boldsymbol{\psi} - \gamma_h(\Pi_h \boldsymbol{\psi})\|_{0,\Omega} + C \|\varphi\|_{0,\Omega} \|\gamma_h(\Pi_h \boldsymbol{\psi}) - \Pi_h \boldsymbol{\psi}\|_{0,\Omega} \\
& \leq Ch \|\boldsymbol{\psi}\|_{0,\Omega} \|\Pi_h \boldsymbol{\psi}\|_{1,h} + Ch \|\varphi\|_{0,\Omega} \|\Pi_h \boldsymbol{\psi}\|_{1,h} \\
& \leq Ch \|\boldsymbol{\psi}\|_{0,\Omega} \|\varphi\|_{0,\Omega} + Ch \|\varphi\|_{0,\Omega}^2 \\
(61) \quad & \leq Ch \|\boldsymbol{\psi}\|_{0,\Omega}^2 + Ch \|\varphi\|_{0,\Omega}^2 + Ch \|\varphi\|_{0,\Omega}^2,
\end{aligned}$$

where the last inequality is obtained from the Cauchy inequality. On each $e \in \Gamma_{h,i}$, since $\bar{\phi}_i$ is a constant, we have

$$\int_e \bar{\phi}_i (\Pi_h \boldsymbol{\psi} - \gamma_h(\Pi_h \boldsymbol{\psi})) \cdot \mathbf{n} ds = \int_e \bar{\phi}_i (\Pi_h \boldsymbol{\psi} - (\Pi_h \boldsymbol{\psi})(M_e)) \cdot \mathbf{n} ds = 0.$$

Therefore,

$$\begin{aligned}
(62) \quad & \sum_{i=1}^n \langle \phi_i, (\Pi_h \boldsymbol{\psi} - \gamma_h(\Pi_h \boldsymbol{\psi})) \cdot \mathbf{n}_i \rangle_i + \sum_{i=1}^n \langle p - \bar{p}_i, (\gamma_h(\Pi_h \boldsymbol{\psi}) - \Pi_h \boldsymbol{\psi}) \cdot \mathbf{n}_i \rangle_i \\
& = \sum_{i=1}^n \langle \phi_i - \bar{\phi}_i, (\Pi_h \boldsymbol{\psi} - \gamma_h(\Pi_h \boldsymbol{\psi})) \cdot \mathbf{n}_i \rangle_i + \sum_{i=1}^n \langle p - \bar{p}_i, (\gamma_h(\Pi_h \boldsymbol{\psi}) - \Pi_h \boldsymbol{\psi}) \cdot \mathbf{n}_i \rangle_i \\
& = \sum_{i=1}^n \langle p_i - \bar{p}_i, (\Pi_h \boldsymbol{\psi} - \gamma_h(\Pi_h \boldsymbol{\psi})) \cdot \mathbf{n}_i \rangle_i + \sum_{i=1}^n \langle p - \bar{p}_i, (\gamma_h(\Pi_h \boldsymbol{\psi}) - \Pi_h \boldsymbol{\psi}) \cdot \mathbf{n}_i \rangle_i \\
& = 0,
\end{aligned}$$

where we have used the fact that $\phi_i - \bar{\phi}_i = (p_i - \lambda_{h,i}) - (\bar{p}_i - \lambda_{h,i})$. For the last term on the right hand side of (57), it is obvious that

$$(\gamma_h(\Pi_h \boldsymbol{\psi}) - \Pi_h \boldsymbol{\psi}, \nabla \varphi) = (\gamma_h(\Pi_h \boldsymbol{\psi}) - \Pi_h \boldsymbol{\psi}, \nabla p).$$

Using (25), (56) and the Young's inequality in above equality, we have

$$\begin{aligned}
& (\gamma_h(\Pi_h \boldsymbol{\psi}) - \Pi_h \boldsymbol{\psi}, \nabla \varphi) \leq Ch \|\Pi_h \boldsymbol{\psi}\|_{1,h} \|\nabla p\|_{0,\Omega} \\
& \leq Ch \|\varphi\|_{0,\Omega} \|\nabla p\|_{0,\Omega} \\
(63) \quad & \leq C\varepsilon \|\varphi\|_{0,\Omega}^2 + \frac{C}{\varepsilon} h^2 \|\nabla p\|_{0,\Omega}^2.
\end{aligned}$$

Substitute (58), (59), (60), (61), (62) and (63) into (57) to obtain

$$\begin{aligned}
& (C - C\varepsilon - Ch) \|\varphi\|_{0,\Omega}^2 + (C - C\varepsilon - Ch) \|\boldsymbol{\psi}\|_{0,\Omega}^2 \\
& \leq \frac{C}{\varepsilon} \|p - \hat{p}\|_{0,\Omega}^2 + \frac{C}{\varepsilon} \|\mathbf{u} - \Pi_h \mathbf{u}\|_{0,\Omega}^2 + \frac{C}{\varepsilon} h^2 \|\nabla p\|_{0,\Omega}^2 - \sum_{i=1}^n \langle \phi_i, \Pi_h \boldsymbol{\psi} \cdot \mathbf{n}_i \rangle_i.
\end{aligned}$$

It is easy to see that there exists a positive constant ε which is independent of h , such that

$$\begin{aligned}
& \|\varphi\|_{0,\Omega}^2 + \|\boldsymbol{\psi}\|_{0,\Omega}^2 \\
(64) \quad & \leq C \|p - \hat{p}\|_{0,\Omega}^2 + C \|\mathbf{u} - \Pi_h \mathbf{u}\|_{0,\Omega}^2 + Ch^2 \|\nabla p\|_{0,\Omega}^2 - \sum_{i=1}^n \langle \phi_i, \Pi_h \boldsymbol{\psi} \cdot \mathbf{n}_i \rangle_i,
\end{aligned}$$

provided sufficiently small h .

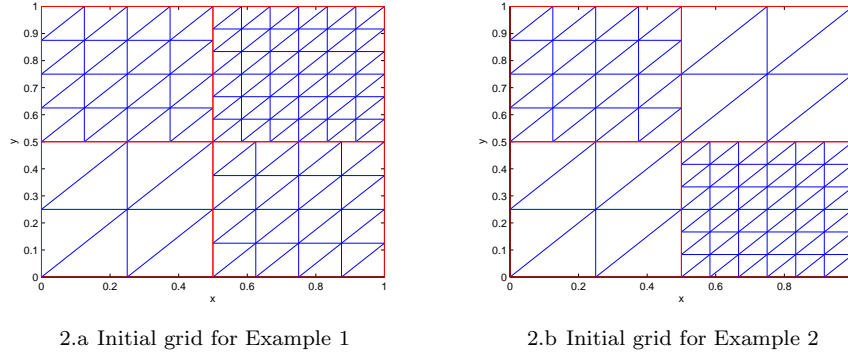


FIGURE 2. Initial grids for Example 1 and Example 2.

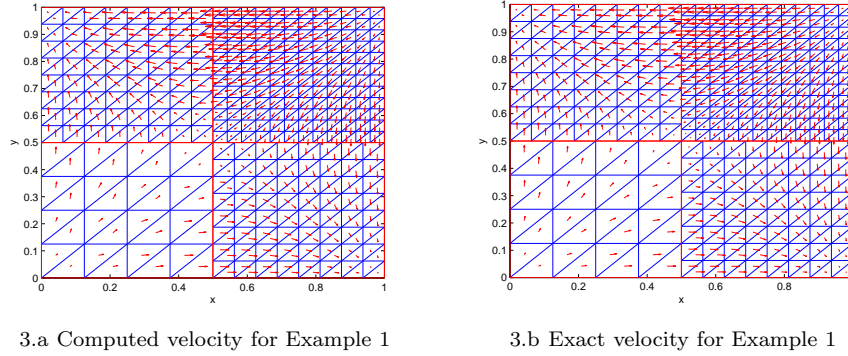


FIGURE 3. Computed velocity and exact velocity for Example 1.

We finally plus (54) and (64) to get

$$\begin{aligned}
 & \| \varphi \|_{0,\Omega}^2 + \| \boldsymbol{\psi} \|_{0,\Omega}^2 + \sum_{i,j=1}^n \alpha \| | \phi_i - \phi_j | \|_{i,j}^2 + \sum_{i,j=1}^n \frac{1}{\alpha} \| | \boldsymbol{\psi}_i \cdot \mathbf{n}_i + \boldsymbol{\psi}_j \cdot \mathbf{n}_j | \|_{i,j}^2 \\
 & \leq C \| p - \hat{p} \|_{0,\Omega}^2 + C \| \mathbf{u} - \Pi_h \mathbf{u} \|_{0,\Omega}^2 + Ch^2 \| \nabla p \|_{0,\Omega}^2 \\
 & + C \left(\alpha \| | p - \bar{p}_i | \|_i^2 + \frac{1}{\alpha} \| | (\mathbf{u} - \Pi_h \mathbf{u}) \cdot \mathbf{n}_i | \|_i^2 \right).
 \end{aligned}$$

From the approximate properties presented in [20], the desired result (35) is obtained immediately. \square

5. Numerical examples

In this section, we report some numerical results yielded by the MFV method proposed in this article. We compare them with the numerical results obtained by the non-mortar MFE method presented in [19]. For simplicity we choose the unit square as the initial domain Ω in all examples, which is divided into four sub-domains with interfaces along the lines $x = 1/2$ and $y = 1/2$. Let h be the maximum grid size in every triangulation. In addition, we define the following norm

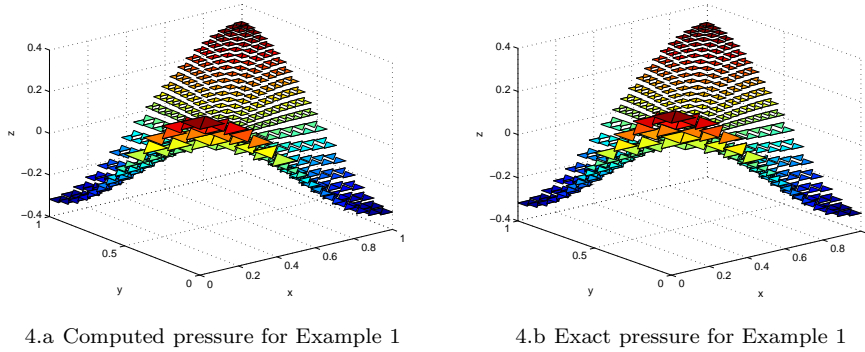


FIGURE 4. Computed pressure and exact pressure for Example 1.

TABLE 1. Errors and convergence rates for Example 1 using the MFE method.

$1/h$	$\ \mathbf{u} - \mathbf{u}_h \ _{0,\Omega}$	Order	$\ p - p_h \ _{0,\Omega}$	Order	$\ p - \lambda_h \ _L$	Order
4	1.3565×10^{-1}	—	5.3189×10^{-2}	—	1.0216×10^{-1}	—
8	6.4991×10^{-2}	1.0615	2.7212×10^{-2}	0.9668	4.5157×10^{-2}	1.1778
16	3.1283×10^{-2}	1.0548	1.3691×10^{-2}	0.9910	2.0516×10^{-2}	1.1382
32	1.5234×10^{-2}	1.0380	6.8512×10^{-3}	0.9987	9.5879×10^{-3}	1.0974
64	7.6110×10^{-3}	1.0147	3.4263×10^{-3}	0.9999	4.6839×10^{-3}	1.0335

to measure the error $p - \lambda_h$:

$$\| p - \lambda_h \|_L = \left(\sum_{i=1}^n \| p_i - \lambda_{h,i} \|^2 \right)^{1/2}.$$

Example 1: We consider the problem (1)-(3) with $\beta(\mathbf{x}) \equiv 0$ and $c(\mathbf{x}) \equiv 1$. The source term $f(x)$ is chosen in such a way that the exact solution and tensor coefficient are

$$p(x, y) = \frac{\cos(\pi x)\cos(\pi y)}{\pi},$$

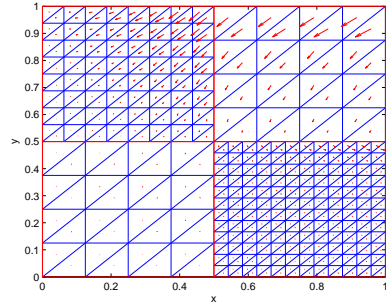
and

$$K(\mathbf{x}) = I, \text{ for } 0 \leq y \leq 1/2, \quad K(\mathbf{x}) = \begin{pmatrix} 2y & 0 \\ 0 & 1 \end{pmatrix}, \text{ for } 1/2 \leq y \leq 1.$$

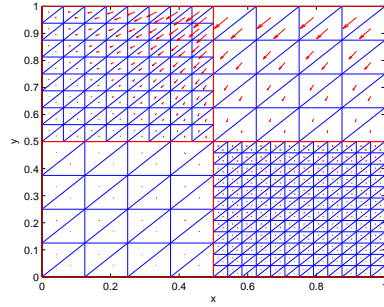
It is easy to find that $K(\mathbf{x})$ is smooth on the whole domain Ω . The initial non-matching grid is shown in Figure 2.a. Numerical errors and convergence rates are presented in Table 2. We note that optimal convergence $O(h)$ is observed for \mathbf{u}_h , p_h and λ_h , which conforms to our theoretical results. From Tables 1 and 2, it can be seen that the MFV method is comparable to the MFE method. The computed solutions and the exact solutions are shown in Figures 3 and 4 for both pressure and velocity.

TABLE 2. Errors and convergence rates for Example 1 using the MFV method.

$1/h$	$\ \mathbf{u} - \mathbf{u}_h\ _{0,\Omega}$	Order	$\ p - p_h\ _{0,\Omega}$	Order	$\ p - \lambda_h\ _L$	Order
4	1.3565×10^{-1}	—	5.3287×10^{-2}	—	1.0230×10^{-1}	—
8	6.4990×10^{-2}	1.0615	2.7220×10^{-2}	0.9691	4.5169×10^{-2}	1.1794
16	3.1282×10^{-2}	1.0548	1.3692×10^{-2}	0.9913	2.0510×10^{-2}	1.1390
32	1.5230×10^{-2}	1.0384	6.8489×10^{-3}	0.9993	9.5800×10^{-3}	1.0982
64	7.6108×10^{-3}	1.0150	3.4109×10^{-3}	1.0057	3.3428×10^{-3}	1.0348



5.a Computed velocity for Example 2



5.b Exact velocity for Example 2

FIGURE 5. Computed velocity and exact velocity for Example 2.

Example 2: Consider the following Dirichlet boundary value problem:

$$(65) \quad \mathbf{u} = -K(\mathbf{x})\nabla p \quad \text{in } \Omega_i,$$

$$(66) \quad \nabla \cdot \mathbf{u} = q \quad \text{in } \Omega_i,$$

$$(67) \quad p|_{\partial\Omega} = g \quad \text{on } \partial\Omega,$$

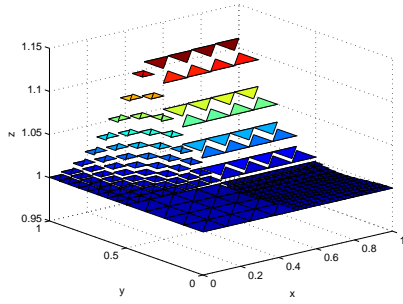
where the exact solution is

$$p(x, y) = \begin{cases} x^2 y^3 + \cos(xy), & 0 \leq x \leq \frac{1}{2}, \\ \left(\frac{2x+99}{200}\right)^2 y^3 + \cos\left(\frac{2x+99}{200}y\right), & \frac{1}{2} \leq x \leq 1, \end{cases}$$

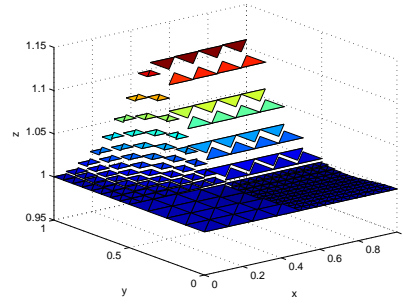
and the coefficient

$$K(\mathbf{x}) = I, \text{ for } 0 \leq x \leq \frac{1}{2}, \quad K(\mathbf{x}) = 100 * I, \text{ for } \frac{1}{2} \leq x \leq 1.$$

In this example, the coefficient $K(\mathbf{x})$ is discontinuous across the interfaces, and the MFV method proposed for problems with Neumann boundary condition is extended to Dirichlet boundary value problems. The initial non-matching grid is shown in Figure 2.b. Numerical errors and convergence rates filled in Tables 3 and 4 indicate that this MFV method on non-matching grid is convergent at $O(h)$ rate for all variables and the computational results of MFE method and MFV method are almost the same. By the stability estimate and the error analysis used in this article, we could get conclusions similar to these in Theorems 4.1 and 4.2, except that there are no terms associated with the pressure. But it can be estimated additionally by the duality argument, we refer readers to [20] for a similar analysis.



6.a Computed pressure for Example 2



6.b Exact pressure for Example 2

FIGURE 6. Computed pressure and exact pressure for Example 2.

TABLE 3. Errors and convergence rates for Example 2 using the MFE method.

$1/h$	$\ \mathbf{u} - \mathbf{u}_h \ _{0,\Omega}$	Order	$\ p - p_h \ _{0,\Omega}$	Order	$\ p - \lambda_h \ _L$	Order
4	7.4465×10^{-2}	—	1.8007×10^{-2}	—	6.7140×10^{-2}	—
8	3.7975×10^{-2}	0.9715	9.1334×10^{-3}	0.9793	3.3782×10^{-2}	0.9909
16	1.7750×10^{-2}	1.0972	4.5832×10^{-3}	0.9947	1.5825×10^{-2}	1.0403
32	7.3916×10^{-3}	1.0638	2.2936×10^{-3}	0.9987	6.9380×10^{-3}	1.1432
64	3.3621×10^{-3}	1.1365	1.1437×10^{-3}	1.0039	3.1464×10^{-3}	1.1408

TABLE 4. Errors and convergence rates for Example 2 using the MFV method.

$1/h$	$\ \mathbf{u} - \mathbf{u}_h \ _{0,\Omega}$	Order	$\ p - p_h \ _{0,\Omega}$	Order	$\ p - \lambda_h \ _L$	Order
4	8.1843×10^{-2}	—	1.8013×10^{-2}	—	7.5458×10^{-2}	—
8	4.1933×10^{-2}	0.9647	9.1342×10^{-3}	0.9796	3.8232×10^{-2}	0.9808
16	1.9528×10^{-2}	1.1025	4.5833×10^{-3}	0.9948	1.8666×10^{-2}	1.0343
32	8.9488×10^{-3}	1.1257	2.2937×10^{-3}	0.9987	8.5317×10^{-3}	1.1295
64	4.1004×10^{-3}	1.1259	1.1466×10^{-3}	1.0003	3.8982×10^{-3}	1.1300

TABLE 5. Errors and convergence rates for Example 3 using the MFE method.

$1/h$	$\ \mathbf{u} - \mathbf{u}_h \ _{0,\Omega}$	Order	$\ p - p_h \ _{0,\Omega}$	Order	$\ p - \lambda_h \ _L$	Order
4	2.1274×10^{-1}	—	4.3351×10^{-2}	—	1.7710×10^{-1}	—
8	1.2550×10^{-1}	0.7614	2.1374×10^{-2}	1.0202	1.0023×10^{-1}	0.8212
16	6.7228×10^{-2}	0.9005	1.0382×10^{-2}	1.0417	5.2904×10^{-2}	0.9218
32	3.4467×10^{-2}	0.9638	5.1334×10^{-3}	1.0160	2.7112×10^{-2}	0.9644
64	1.7264×10^{-2}	0.9974	2.5489×10^{-3}	1.0100	1.3706×10^{-2}	0.9841

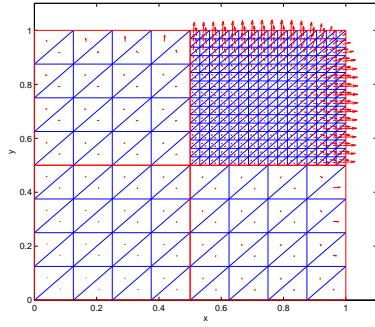
Example 3: We consider the problem (65)-(67) with $K(\mathbf{x}) = I$ and the source term q is chosen in such a way that the exact solution is

$$p(x, y) = bx(e^{ax} - e^a)y(e^{ay} - e^a), \quad a = 10, \quad b = 0.90909 \times 10^{-9}.$$

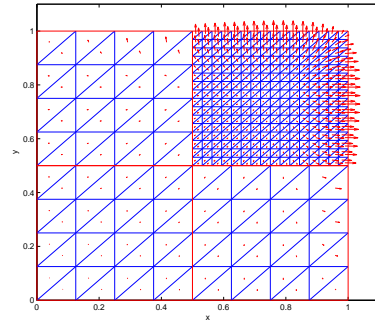
This solution obviously changes substantially in the upper right corner of the domain Ω . Therefore, we apply a locally refined grid as the initial grid, on which the

TABLE 6. Errors and convergence rates for Example 3 using the MFV method.

$1/h$	$\ \mathbf{u} - \mathbf{u}_h \ _{0,\Omega}$	Order	$\ p - p_h \ _{0,\Omega}$	Order	$\ p - \lambda_h \ _L$	Order
4	2.1320×10^{-1}	—	4.5729×10^{-2}	—	1.7627×10^{-1}	—
8	1.2556×10^{-1}	0.7638	2.1860×10^{-2}	1.0648	1.0008×10^{-1}	0.8166
16	6.7236×10^{-2}	0.9010	1.0456×10^{-2}	1.0639	5.2885×10^{-2}	0.9202
32	3.4468×10^{-2}	0.9639	5.1435×10^{-3}	1.0235	2.7109×10^{-2}	0.9640
64	1.7273×10^{-2}	0.9967	2.5310×10^{-3}	1.0230	1.3700×10^{-2}	0.9845

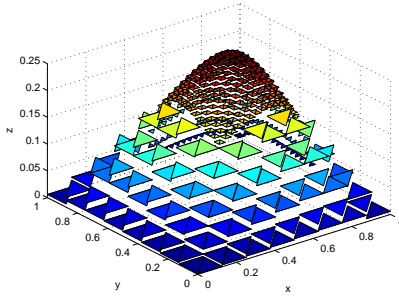


7.a Computed velocity for Example 3

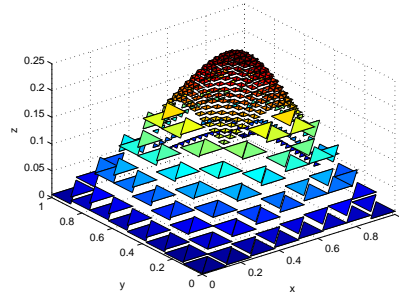


7.b Exact velocity for Example 3

FIGURE 7. Computed velocity and exact velocity for Example 3.



8.a Computed pressure for Example 3



8.b Exact pressure for Example 3

FIGURE 8. Computed pressure and exact pressure for Example 3.

grid on the upper-right sub-domain is four times finer than the rest of the grids. The numerical results for both MFE method and MFV method are summarized in Tables 5 and 6, respectively. The pressures and velocities on the first level of refinement are shown in Figures 7 and 8.

6. Conclusion

In this paper, we have developed a mixed finite volume scheme on non-matching multi-block triangular grid which is an extension of the non-mortar mixed finite element method, see [19]. We verify the scheme has the optimal convergence rates

in L^2 -norm for velocity and pressure under some suitable assumptions on both the coefficients in original equations and the regularity of the exact solutions. The numerical results provided in last section not only confirm our theoretical analysis, but also indicate this MFV method has almost the same computational efficiency as the non-mortar mixed finite element method.

Acknowledgments

This work of the first author was partially supported by the National Natural Science Foundation of China (Grant No. 11371170). This work of the second author was partially supported by the National Natural Science Foundation of China (Grant No. 11126040), and the National Natural Science Foundation of China (Grant No. 11301214).

References

- [1] B. Ganis, M.F. Wheeler, I. Yotov, An enhanced velocity multipoint flux mixed finite element method for Darcy flow on non-matching hexahedral grids, *Procedia Computer Science* 51 (2015) 1198-1207.
- [2] C.J. Bi, Superconvergence of mixed covolume method for elliptic problems on triangular grids, *J. Comput. Appl. Math.* 216 (2008) 534-544.
- [3] D. Vassilev, C.Q. Wang, I. Yotov, Domain decomposition for coupled Stokes and Darcy flows, *Comput. Methods Appl. Mech. Engrg.* 268 (2014) 264-283.
- [4] F. Brezzi, M. Fortin, *Mixed and Hybrid Finite Element Methods*, Springer-Verlag, New York, 1991.
- [5] H.X. Rui, R. Zhang, A unified stabilized mixed finite element method for coupling Stokes and Darcy flows, *Comput. Methods Appl. Mech. Engrg.*, 198 (2009) 2692-2699.
- [6] H.X. Rui, Superconvergence of a Mixed Covolume Method for Elliptic Problems, *Computing* 71 (2003) 247-263.
- [7] H.X. Rui, T.C. Lu, An Expanded Mixed Covolume Method for Elliptic Problems, *Numerical Methods for P.D.E.* 21 (2005) 8-23.
- [8] H.X. Rui, Convergence of an upwind control-volume mixed finite element method for convection-diffusion problems. *Computing* 81 (2007) 297-315.
- [9] I.D. Mishev, Analysis of a new mixed finite volume method, *Comput. Methods Appl. Math.* 3 (2003) 189-201.
- [10] J.A. Wheeler, M.F. Wheeler, I. Yotov, Enhanced velocity mixed finite element methods for flow in multiblock domains, *Comput. Geosci.* 6 (2002) 315-332.
- [11] J.L. Lv, Y.H. Li, Optimal biquadratic finite volume element methods on quadrilateral meshes, *SIAM J. Numer. Anal.* 50 (2012) 2379-2399.
- [12] P.G. Ciarlet, P.A. Raviart, J.L. Lions, General Lagrange and Hermite Interpolation in \mathbb{R}^n with applications to Finite Element Methods, *Arch. Rat. Mech. Anal.* 46 (1972) 177-199.
- [13] S.C. Brenner, L.R. Scott, *The Mathematical Theory of Finite Element Methods*, Texts in Appl. Math. 15(2008).
- [14] S.G. Thomas, M.F. Wheeler, Enhanced velocity mixed finite element methods for modeling coupled flow and transport on non-matching multiblock grids, *Comput. Geosci.* 15 (2011) 605-625.
- [15] S.H. Chou, D.Y. Kwak, P.S. Vassilevski, Mixed covolume methods for elliptic problems on triangular grids, *SIAM J. Numer. Anal.* 35 (1998) 1850-1861.
- [16] S.H. Chou, D.Y. Kwak, K.Y. Kim, A general framework for constructing and analyzing mixed finite volume methods on quadrilateral grids: the overlapping covolume case, *SIAM J. Numer. Anal.* 39 (2001) 170-1196.
- [17] S.H. Chou, D.Y. Kwak, K.Y. Kim, Mixed finite volume methods on nonstaggered quadrilateral grids for elliptic problems, *Math. Comput.* 72 (2003) 525-539.
- [18] T. Arbogast, H.L. Xiao, Two-level mortar domain decomposition preconditioners for heterogeneous elliptic problems, *Comput. Methods Appl. Mech. Engrg.* 292 (2015)221-242.
- [19] T. Arbogast, I. Yotov, A non-mortar mixed finite element method for elliptic problems on non-matching multiblock grids, *Comput. Methods Appl. Mech. Engrg.* 149 (1997) 255-265.
- [20] T. Arbogast, L.C. Cowsar, M.F. Wheeler, I. Yotov, Mixed finite element methods on non-matching multiblock grids, *SIAM J. Numer. Anal.* 37 (2000) 1295-1315.

- [21] V. Girault, D. Vassilev, I. Yotov, Mortar multiscale finite element methods for Stokes-Darcy flows, *Numer. Math.* 127 (2014) 93-165.
- [22] W.F. Tian, Y.H. Li, Superconvergence of mixed covolume method on quadrilateral grids for elliptic problems, *J. Syst. Sci. Complex.* 25 (2012) 385-397.
- [23] W.F. Tian, L.Q. Song, Y.H. Li, A stabilized equal-order finite volume method for the stokes equations, *J. Comput. Math.* 30 (2012) 615-628.
- [24] X. Tunc, I. Faille, T. Gallouët, M.C. Cacas, P. Havé, A model for conductive faults with non-matching grids, *Comput. Geosci.* 16 (2012) 277-296.
- [25] X.K. Zhao, Y.L. Chen, J.L. Lv, A mixed nonoverlapping covolume method on quadrilateral grids for elliptic problems, *J. Comput. Appl. Math.* 292 (2016) 23-40.

College of Mathematics, Jilin University, Changchun 130012, Jilin, People's Republic of China
E-mail: gaoyan10@163.com(Y.N. Gao) and lvjl@jlu.edu.cn(J.L. Lv)